
A Unifying Lens on Supervised Fine-Tuning Through Target Distribution Design

Tong Xie¹ Yuanhao Ban^{1,2} Yunqi Hong¹ Sohyun An¹ Yihang Chen¹ Cho-Jui Hsieh^{1,2}

¹University of California, Los Angeles (UCLA), ²Arena
 {tongxie,chohsieh}@cs.ucla.edu

Project Page:  **Target-SFT**

Abstract

Supervised fine-tuning (SFT) typically maximizes the likelihood of every token in a demonstrated trajectory. However, an observed token can be non-unique, noisy, or misaligned with the model prior. Strictly fitting toward this one-hot target may be suboptimal, especially when the pretrained model encodes a rich knowledge prior. In this work, we reinterpret SFT as target distribution design: instead of studying only the loss objective, we analyze the token-level target that the loss drives the model to match. We introduce the Q -target framework, which decomposes SFT supervision into two explicit choices: (1) **how strongly to rely on the observed token**, and (2) **how to allocate the remaining probability mass** over alternatives. This perspective unifies many existing SFT variants as implicit choices of the target distribution Q . Building on this view, we propose TARGET-SFT which constructs the training objective directly from the desired target distribution. This method consistently outperforms across the ten reasoning dataset-model settings evaluated, showing the effectiveness of this target-based approach. Overall, our formulation reveals a more fundamental design principle for SFT training and opens a broader search space for SFT objectives.

1 Introduction

Supervised fine-tuning (SFT) is a central stage in the post-training of large language models (LLMs) [1, 2, 3]. By imitating expert behaviors, SFT enables the pretrained model to acquire new knowledge and adapt to tasks efficiently. Despite its popularity, standard SFT relies on a particularly rigid form of supervision, by training the model toward a one-hot target distribution: at every token position, SFT maximizes the probability of the demonstrated token y_t , while all other tokens are assigned zero probability. This formulation implicitly assumes that every observed token in the dataset is an ideal and uniquely correct target.

This one-hot view reveals a limitation of standard SFT, especially in post-training settings [4, 5, 6]. In realistic SFT data, an observed token is rarely the only valid continuation. The same prompt may admit multiple correct reasoning paths, phrasings, intermediate steps, or stylistic choices [7, 8, 9, 10, 11, 12]. At the same time, the model already encodes a rich prior from pretraining [6, 13, 11]. In such cases, forcing the model to strictly imitate every token can amplify noise, induce overconfidence, interfere with the pretrained model prior, and degrade generalization [14, 15, 16, 17, 18]. A growing line of work relaxes the SFT supervision by modifying the objective, for example, through token-level importance reweighting [13, 11, 19, 20] or regularization [5, 17, 21, 22]. While these approaches are effective, they are often presented as separate algorithmic choices. It remains unclear the connection between variants and how to construct better SFT objectives.

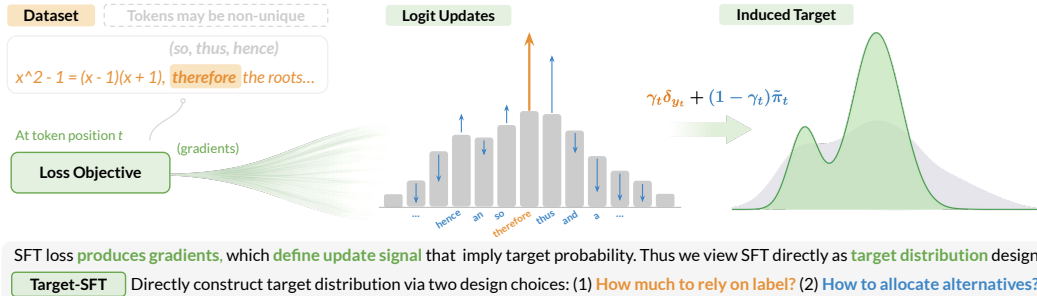


Figure 1: **Overview.** An SFT loss drives the model to match an implicitly defined target distribution. This view motivates TARGET-SFT that designs the SFT target directly. It also offers a unifying lens, where many SFT variants can be viewed as different target designs through the choices of γ_t and $\tilde{\pi}_t$.

In this work, we propose a different perspective: rather than the loss, we ask what **target distribution** should SFT drive the model to learn. This is more fundamental than the choice of loss alone, because loss is merely an optimization surrogate, while the target distribution directly specifies the desired allocation of probability mass (Figure 1). By viewing SFT as target distribution design, we can control the supervision signal when the observed label y_t is suboptimal: If y_t is ideal and unique, the target should be close to the one-hot distribution δ_{y_t} , maximizing its probability. If it is noisy or misaligned with the model prior, then the target should soften supervision and allocate probability to alternatives. Building on this intuition, we introduce a Q -target distribution framework for SFT:

$$Q_t = \gamma_t \delta_{y_t} + (1 - \gamma_t) \tilde{\pi}_t,$$

where $\gamma_t \in [0, 1]$ controls the target probability assigned to the observed token y_t based on uncertainty, and $\tilde{\pi}$ specifies the plausible alternatives for the $1 - \gamma_t$ residual probability mass. This perspective thus reveals two key questions through the choices of $(\gamma_t, \tilde{\pi}_t)$: (1) **how much to rely on the observed token y_t** , and (2) **where to allocate the remaining probability mass when y_t is uncertain?**

In particular, we show that many existing SFT variants can be understood as varying ways of answering these two questions, and seemingly different losses correspond to implicit choices of target distribution Q . Based on this insight, we propose TARGET-SFT by explicitly leveraging the structure revealed by the Q -framework, which previous methods have largely left implicit. In general, we argue that the fundamental object in SFT is not the loss function itself, but the target distribution induced by the loss. This Q -target perspective provides a unifying lens in SFT objective design, and exposes a general design space for balancing dataset imitation, prior preservation, and alternative supervision. Our contributions are as follows:

1. We introduce a target-distribution perspective on SFT, showing that arbitrary token-level SFT losses can be understood through the induced target distributions they drive the model to learn.
2. We propose the Q -target framework, which unifies existing SFT variants by decomposing objective design into two explicit choices: how much to rely on the observed token and how to allocate the remaining probability mass.
3. We propose TARGET-SFT as a concrete instantiation motivated by the Q -target view, and empirically validate its performance across 10 dataset-model settings.

2 Related Work

Existing works improve SFT along three main directions. We organize them under the Q -target lens, which characterizes SFT variants by how they specify the effective token-level target distribution. We include the concrete connection for representative methods in Appendix C.

Token-level Reweighting. Standard SFT applies uniform cross-entropy updates to all tokens, treating every token as equally reliable. Token-reweighting methods challenge this assumption by changing how strongly each token contributes to training. DFT [13], beyond-log [6], and ProFit [11] use the model probability on the observed token to rescale or filter updates, focusing on tokens that

are compatible with the model prior. EAFT [20] uses entropy-based uncertainty to reduce potentially destructive updates; iw-SFT [23] and CFT [19] assign weights based on trajectory- or token-level quality. These methods primarily address the *choice of γ_t in SFT target construction*, controlling how much target mass should be assigned to the observed label. However, reweighting the one-hot loss only weakens or strengthens imitation, but leaves the remaining probability mass underspecified. Our framework provides a complete view by making the effective training target explicit.

Distribution-level Prior. Another line of work introduces soft distributional signals beyond the one-hot label. Reference-constrained methods such as ASFT [21], RL’s Razor [15], and Proximal SFT [22] regularize updates to prevent large drift from a reference model. Huang et al. [17] uses label-smoothing to address overconfidence. GEM [5] uses reverse KL and entropy regularization to preserve output diversity and reduce forgetting. These methods address the rigidity in strict one-hot imitation, proposing alternative sources for probability allocation. They mainly specify the *choice of $\tilde{\pi}$, allocating probability mass to non-observed alternatives*: KL-constraints allocate toward the reference model, label smoothing allocates toward a uniform prior, and diversity-preserving methods discourage collapse onto a narrow set of tokens.

Dataset-level Curations. A complementary direction improves SFT by changing the training trajectories. Prior work has proposed augmenting demonstrations with multiple valid trajectories [9, 24], filtering examples by quality [25, 26], and using model-generated or model-aligned responses [16]. GRAPE [18] selects trajectories with high likelihood under the model, while rejection-sampling fine-tuning trains on correct model-generated responses [9, 27, 28, 29]. Self-distillation fine-tuning [30] projects expert demonstrations into the model’s distributional style, reducing data-model mismatch. These approaches address the same underlying issue as our work: the demonstrated trajectory or token may not be uniquely ideal for the model to imitate. By improving the dataset, they indirectly change the effective target distribution seen during SFT. In contrast, our work remains on the objective level and directly designs the effective target distribution for a fixed dataset.

3 Preliminary

Supervised Fine-Tuning. Let \mathcal{D} be a supervised dataset of pairs $(x, y) \sim \mathcal{D}$, where x is the input prompt and $y = (y_1, \dots, y_T)$ is the demonstrated response sequence. Given the prefix $x_t = (x, y_{<t})$, a language model defines the next-token distribution $\pi_\theta(\cdot | x_t) \in \Delta^{|\mathcal{V}|}$ over the vocabulary \mathcal{V} .

Standard SFT minimizes the token-level negative log-likelihood:

$$\mathcal{L}_{\text{SFT}}(\theta) = \mathbb{E}_{(x,y) \sim \mathcal{D}} \left[- \sum_{t=1}^T \log \pi_\theta(y_t | x_t) \right].$$

Target Distribution. Equivalently, let δ_{y_t} denote the one-hot vector that assigns probability 1 to the observed token y_t and 0 to all other tokens, $\delta_{y_t}(v) = \mathbf{1}\{v = y_t\}$. Then the objective can be written as the cross-entropy with target δ_{y_t} as $\mathcal{L}_{\text{SFT}}(\theta) = \mathbb{E}_{(x,y) \sim \mathcal{D}} \sum_{t=1}^T \text{CE}(\delta_{y_t}, \pi_\theta(\cdot | x_t))$.

4 Q-Target Framework for SFT

The one-hot target δ_y in SFT implicitly assumes that y_t is the single optimal continuation for the prefix x_t . However, an observed token can be non-unique, noisy, or distributionally mismatched with the model prior. To capture this, we relax the assumption and account for the uncertainty in y_t , constructing a new target distribution Q_t in place of δ_y .

4.1 Modeling Latent Trust

We introduce a latent binary variable to represent whether the observed token should be strictly imitated. Let $Z_t \in \{0, 1\}$ be where $Z_t = 1$ indicates y_t is strictly trusted as the target, and $Z_t = 0$ indicates that supervision should relax to a broader distribution over plausible alternatives. Under this view, the ideal target distribution can be written as

$$P(\cdot | x_t) = P(Z_t = 1 | x_t) \delta_{y_t} + P(Z_t = 0 | x_t) \tilde{\pi}_t(\cdot | x_t), \tag{1}$$

where $\tilde{\pi}_t \in \Delta^{|\mathcal{V}|}$ denotes an alternative distribution over plausible next tokens.

Since Z_t is unobserved, the trust probability $r_t = P(Z_t = 1 \mid x_t)$ is unknown. We model this uncertainty using a Beta distribution:

$$r_t \sim \text{Beta}(\alpha_t, \beta_t),$$

where α_t is evidence supporting y_t , and β_t is evidence that y_t may be non-unique or should relax toward alternatives. The posterior mean $\gamma_t = \mathbb{E}[r_t] = \frac{\alpha_t}{\alpha_t + \beta_t} \in [0, 1]$ then gives the expected trust for the observed token y_t .

Taking expectation over Eq. (1) leads to the ideal target distribution

$$Q_t = \mathbb{E}_{r_t}[P(\cdot \mid x_t)] = \gamma_t \delta_{y_t} + (1 - \gamma_t) \tilde{\pi}_t. \quad (2)$$

Intuitively, the target probability for y_t is scaled by the expected trust γ_t in the token, and the residual probability mass is reallocated to plausible alternatives over $\tilde{\pi}_t$.

4.2 Final Target & Objective

We replace the SFT one-hot target with Q_t , and train with the cross-entropy loss:

$$\mathcal{L}_Q(\theta) = \mathbb{E}_{(x,y) \sim \mathcal{D}} \sum_{t=1}^T \text{CE}(Q_t, \pi_\theta(\cdot \mid x_t)).$$

Proposition 1 (Token-level decomposition of Q -target training). Given the target distribution Q_t defined in Eq. (2), the token-level cross-entropy loss at position t decomposes as

$$\text{CE}(Q_t, \pi_\theta(\cdot \mid x_t)) = \gamma_t \text{CE}(\delta_{y_t}, \pi_\theta(\cdot \mid x_t)) + (1 - \gamma_t) \text{CE}(\tilde{\pi}_t, \pi_\theta(\cdot \mid x_t)). \quad (3)$$

This shows that training to match the Q -target involves two forms of supervision: (1) **label imitation**, which pushes the model toward the observed token y_t , with strength controlled by the expected trust γ_t , and (2) **residual distribution matching**, which assigns the remaining supervision mass to alternatives through $\tilde{\pi}_t$. See Appendix B.1 for proof.

5 Unifying Perspective

5.1 Existing Variants

The Q -target formulation separates token-level supervision into two design choices: (1) $\gamma_t \in [0, 1]$ controls the target probability mass on y_t , while (2) $\tilde{\pi}_t \in \Delta^{|\mathcal{V}|}$ specifies how the residual probability is allocated. We show that this view unifies many existing SFT variants. Table 4 provides details of each variant discussed, and Table 5 summarizes their interpretation under Q -target framework.

Standard SFT. Consider the degenerate choice $\gamma_t = 1$, then the Q -objective in Eq. (3) reduces to the negative log-likelihood in SFT, corresponding to setting $Q_{t,k} = \delta_{y_t}$:

$$\text{CE}(Q_t, \pi_\theta) = \text{CE}(\delta_{y_t}, \pi_\theta) = -\log \pi_\theta(y_t \mid x_t), \quad Q_t(k) = \delta_{y_t}(k) = \begin{cases} 1, & k = y_t, \\ 0, & k \neq y_t. \end{cases}$$

Hence, standard SFT is the special case that places full probability on every observed token y_t and assigns no residual mass to alternatives.

Token-Weighted Variants. A class of SFT variants modifies the objective by scaling the negative log-likelihood with a detached, per-token importance weight w_t [6, 11, 13, 19, 20, 23]:

$$\mathcal{L}_t = -w_t \log \pi_\theta(y_t \mid x_t),$$

where w_t may depend on model confidence, entropy, sample quality, or other token-level statistics.

Corollary 1 (Token weighting as self-residual Q -target). Assume $w_t \in [0, 1]$ is detached from the current update. The token-weighted loss above corresponds to the choice

$$(\gamma_t = w_t, \tilde{\pi}_t = \text{sg}[\pi_\theta(\cdot \mid x_t)]) \implies Q_t = w_t \delta_{y_t} + (1 - w_t) \text{sg}[\pi_\theta(\cdot \mid x_t)].$$

where $\text{sg}[\cdot]$ denotes the stop-gradient operator. In particular, the residual branch $\tilde{\pi}_t$ is a *self-matching* term that contributes no gradient. See Appendix B.2 for proof.

This shows that token-weighted variants primarily specify γ_t , proposing statistics to determine how strongly to imitate the observed token. And the residual mass $1 - \gamma_t$ is allocated to the current model prior $\text{sg}[\pi_\theta(\cdot | x_t)]$, providing no corrective supervision toward potential alternatives.

Distributional Variants. Another class of SFT variants incorporates distributional signals beyond the observed token [5, 17, 21, 22, 31]. With various intended goals (e.g., to regularize model drift, calibrate confidence, preserve output diversity, etc), these methods enrich hard-label imitation using another distribution target q_t . The objective is of the form

$$\mathcal{L}_t = -a_t \log \pi_\theta(y_t | x_t) + b_t \text{CE}(q_t, \pi_\theta), \quad a_t, b_t \geq 0. \quad (4)$$

Corollary 2 (Distributional variants as residual Q -targets). Given a detached, auxiliary or reference distribution $q_t \in \Delta^{|\mathcal{V}|-1}$, distributional variants correspond to Q -target training with

$$\gamma_t = \frac{a_t}{a_t + b_t}, \quad \tilde{\pi}_t = q_t, \quad \implies \quad Q_t = \gamma_t \delta_{y_t} + (1 - \gamma_t) \tilde{\pi}_t, \quad (5)$$

up to a global constant $a_t + b_t$. Therefore, these methods primarily specify the residual branch $\tilde{\pi}_t$, deciding where non-label probability should be allocated. The relative strength γ_t between label imitation and residual matching is determined by fixed hyperparameter. See Appendix B.3 for proof.

In summary, token-weighted variants mainly design the label-trust coefficient γ_t , while distributional variants design the residual distribution $\tilde{\pi}_t$. Together, they present the two axes in our framework: how strongly to imitate the observed token, and how to allocate the remaining probability mass.

Remark. This is a natural view because an SFT loss is a training surrogate. Although variant losses may take different algebraic forms, their effect on the model is mediated through the probability update over the vocabulary. The loss expression is therefore only a way to generate gradients; the induced target distribution reveals what those gradients effectively drive the model to match. In this sense, the Q -target formulation is a more fundamental perspective beyond the loss forms. This view not only unifies variants but provides a direct lens into training signals. We now formalize this idea, where we derive the induced target Q_t for any arbitrary differentiable token-level loss.

5.2 From Any Loss to Q

An SFT loss defines a surrogate for shaping the model’s next-token distribution. At each prefix x_t , the model outputs a distribution $p_t = \pi_\theta(\cdot | x_t)$, and the loss produces gradients that determine how this probability changes across tokens. Therefore, for any differentiable token-level loss, we can ask *what target probability distribution Q_t does the loss drive the model to match through its gradients?*

Given token position t (notation omitted for clarity), consider the cross-entropy toward target Q_t

$$\mathcal{L}_{\text{CE}}(Q, p) = - \sum_{k \in \mathcal{V}} Q_k \log p_k.$$

Let z denote the logits. The gradient with respect to the k -th logit is simply the prediction difference

$$\frac{\partial \mathcal{L}_{\text{CE}}}{\partial z_k} = p_k - Q_k.$$

This relationship can be inverted. Given any differentiable token-level loss $\mathcal{L}(z, x)$ with logit gradient $g_k = \frac{\partial \mathcal{L}}{\partial z_k}$, we can derive its induced target as

$$Q_k := p_k - g_k. \quad (6)$$

This Q is the target whose cross-entropy gradient $\nabla_z \text{CE}(Q, p) = \nabla_z \mathcal{L}$, aligning exactly with the logit updates produced by \mathcal{L} . It therefore explicitly reveals the training signal encoded by the loss. Appendix D shows example derivations, and visualizes loss through its gradients and target Q .

6 TARGET-SFT

The Q -formulation turns SFT supervision from a static log-likelihood objective into a problem of target distribution design: (1) how much to rely on the observed token y_t , and (2) how to allocate the remaining probability mass. We now introduce TARGET-SFT, which leverages both branches of this construction. We first use a model-based proxy to estimate label uncertainty, and motivate for an external teacher distribution to enrich supervision signals through the residual branch.

Probability-Proxy for γ_t . The ideal target in Eq (2) involves an expected trust $\gamma_t = \mathbb{E}[r_t] = \frac{\alpha_t}{\alpha_t + \beta_t}$, where α_t, β_t represent evidence (such as an empirical count) for the binary event y_t being selected given prefix x_t . However, such a count is intractable in SFT.

Instead, the model probability $p_y = \pi_\theta(y_t | x_t)$ arises as a natural proxy for α_t , which encapsulates statistical evidence accumulated during pretraining. Here p_y represents the fraction of the model’s belief assigned to y_t among all possible continuations. By defining the evidence as $\alpha_t = p_y$ and $\beta_t = 1 - p_y$, the posterior mean resolves to

$$\gamma_t = \frac{p_y}{p_y + (1 - p_y)} = p_y.$$

This derivation motivates probability-weighted SFT variants (such as p -loss) [13, 6], as scaling the SFT target by p_y equates to using predictive probability as proxy measure of uncertainty in the label.

Teacher-Guided Reward Shaping $\tilde{\pi}$. Under the Q -target view, such objectives implicitly use a *self-matching* residual, $\tilde{\pi}_t = \text{sg}[\pi_\theta(\cdot | x_t)]$, as derived in Section 5.1. This shows that as $p_y \rightarrow 0$, the supervision weakens and provides no further corrective gradient. This is limiting because a small p_y may arise from uncertainty in label, or indicate the lack of knowledge where SFT is intended to teach. A purely self-prior residual treats both cases the same, by reducing the imitation strength and providing no additional guidance over plausible alternatives.

This motivates a residual distribution that remains anchored to the model prior, but also allows external corrective signals. To this end, we construct a teacher-guided $\tilde{\pi}_t$. The goal is to preserve model prior without being constrained by it, enabling supervision from teacher-supported alternatives.

We construct $\tilde{\pi}_t$ through KL-regularized reward shaping:

$$\tilde{\pi} = \arg \max_{q \in \Delta} [\mathbb{E}_{a \sim q}[r(a)] - \tau \text{KL}(q || \pi_\theta)],$$

which stays close to π_θ while the reward r specifies the alternative tokens to be upweighted. Let $\pi_T(\cdot | x_t)$ denote a teacher distribution. To incorporate teacher guidance, we define reward using the teacher log-probability, $r(a) = \lambda \log \pi_T(a)$.

The solution has the form $\tilde{\pi}(a) \propto \pi_\theta(a) \exp(r(a)/\tau)$, and substituting the teacher reward yields

$$\tilde{\pi}(a) \propto \pi_\theta(a) \pi_T(a)^\eta, \quad \eta = \lambda/\tau.$$

This results in a teacher-guided $\tilde{\pi}$ close to π_θ , while upweighting alternatives favored by the teacher through token-level reward. For easier interpretation, we consider the closely related form

$$\tilde{\pi}_t^{\text{guided}}(a) \propto \pi_\theta(a | x_t)^{1-\eta} \pi_T(a | x_t)^\eta, \quad \eta \in [0, 1].$$

It interpolates between the student ($\eta \rightarrow 0$) and teacher distribution ($\eta \rightarrow 1$). This parameterization is convenient in practice, since η directly controls the intensity of teacher signals.

TARGET-SFT. Combining the probability-proxy for trust estimate $\gamma_t = p_y$ and the teacher-guided residual distribution $\tilde{\pi} = \tilde{\pi}_{\text{guided}}$ gives the following target:

$$Q_t^{\text{TARGET}} = p_y \delta_{y_t} + (1 - p_y) \tilde{\pi}_t^{\text{guided}}. \quad (7)$$

The corresponding token-level objective decomposes as

$$\text{CE}(Q_t^{\text{TARGET}}, \pi_\theta) = p_y \text{CE}(\delta_{y_t}, \pi_\theta) + (1 - p_y) \text{CE}\left(\tilde{\pi}_t^{\text{guided}}, \pi_\theta\right). \quad (8)$$

TARGET-SFT adaptively balances strict imitation and prior preservation. When the observed token y_t is well-supported by the model, the objective approaches standard SFT. When y_t is uncertain, it weakens one-hot fitting and instead assigns a higher weight to the teacher-guided residual branch. In this regime, teacher supervision acts as a *fallback supervision* that (1) avoids overfitting to uncertain labels, and (2) strengthens signals when a desired token is under-supported by student due to low p_y .

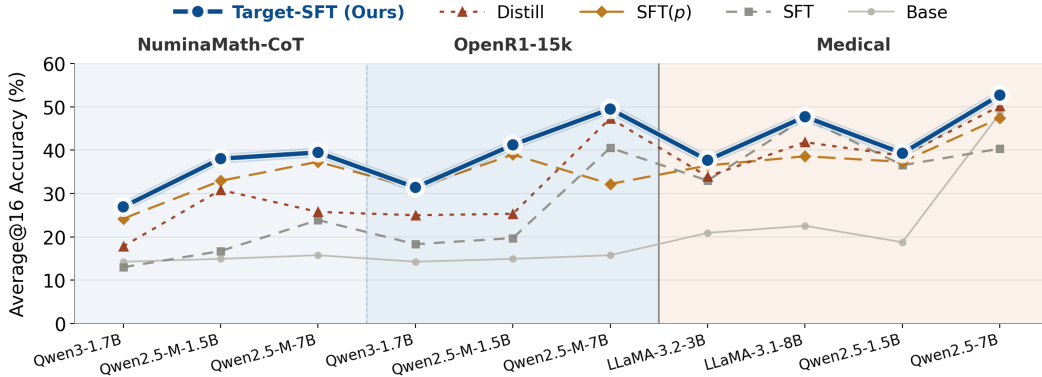


Figure 2: **Performance Summary.** Average@16 accuracy across all 10 dataset-model settings used.

7 Experiments

7.1 Setup

For mathematical reasoning, we train on two datasets: **NuminaMath-CoT-67k** [32, 6] and **OpenR1-Math-15k** [33, 34]. For broader scientific reasoning, we train on **m23k** [35], a high-quality medical reasoning dataset. Our experiments cover across seven diverse models: Qwen2.5 (1.5B & 7B), Qwen2.5-Math (1.5B & 7B), Qwen3-1.7B-Base, LLaMA-3.2-3B, LLaMA-3.1-8B.

We compare TARGET-SFT against the following baselines: (1) **SFT**, which trains with the standard negative log-likelihood. (2) **SFT (p -loss)** [6, 13], a probability-weighted variant that scales loss by the model probability on the observed token. (3) **Knowledge Distillation** [36], which applies teacher distribution on the data as supervision. We use the standard form $\mathcal{L}_{\text{Distill}} = c \text{CE}(\pi_T, \pi_\theta) + (1 - c) \text{CE}(\delta_{y_t}, \pi_\theta)$, where c is constant and ablated in Table 6. These baselines correspond to different partial choices in the Q -target design space: SFT uses the one-hot target, SFT (p) uses $\gamma_t = p_{y_t}$, and KD uses the full teacher distribution as a fixed distributional signal. TARGET-SFT considers both $(\gamma_t, \tilde{\pi}_t)$ and adaptively balances label imitation and the residual branch based on uncertainty in label.

For models that involve teacher distribution, we use the corresponding instruction-tuned model as the teacher; for example, Qwen2.5-1.5B uses Qwen2.5-1.5B-Instruct. For the Qwen3 series, we use Qwen3-4B-Instruct-2507 as the teacher. The evaluation performance is measured by Average@16 accuracy. Further details of evaluation and training configurations are provided in Appendix A.

7.2 Main Results

Across all evaluations, TARGET-SFT achieves the highest Average@16 accuracy. Figure 2 summarizes the results across tasks. While the baselines each show complementary strengths and weaknesses in different dataset-model settings, TARGET-SFT consistently gives the best results. This highlights the value of the structure exposed by the Q -target framework: effective SFT can arise from carefully designing both the imitation strength and the allocation of remaining probability mass.

Math. Table 1 reports the results on NuminaMath-CoT and OpenR1-15k. TARGET-SFT achieves the highest average accuracy across all models on both datasets. In contrast, standard SFT yields only modest gains over the base model in many cases, and even hurts performance for Qwen3-1.7B on NuminaMath-CoT (14.26 \rightarrow 12.99). This is consistent with prior observations that rigid one-hot matching can be limiting for mathematical reasoning [6, 9, 24, 28]. The relatively strong performance of probability-weighted SFT (p -loss) further suggests that reducing imitation strength on uncertain tokens is beneficial. However, TARGET-SFT improves over the p -loss in every case. This supports our claim that choosing γ_t alone and defaulting the residual mass to model prior is incomplete. By explicitly designing $\tilde{\pi}_t$, TARGET-SFT enhances the supervision and achieves stronger performance.

Direct distillation, which uses teacher distribution as the full target, performs relatively weakly on mathematical reasoning. On NuminaMath-CoT, distillation is only slightly better than standard SFT

Table 1: **Mathematical Reasoning.** Average@16 accuracy on five standard benchmarks, using models trained on NuminaMath-CoT (top) and OpenR1 (bottom).

	Minerva Math	Olympiad Bench	AIME24	AMC23	Math500	Avg.
<i>Dataset: NuminaMath-CoT</i>						
Qwen3-1.7B-Base						
Base	9.87	11.35	0.62	16.25	33.81	14.26
SFT	10.78	8.64	0.00	10.78	34.61	12.99
SFT (p)	<u>18.91</u>	<u>17.81</u>	1.24	<u>27.66</u>	<u>53.86</u>	<u>24.20</u>
Distill	14.08	11.92	1.65	19.69	41.52	17.81
TARGET-SFT	21.44	19.21	3.94	30.78	57.55	26.93
Qwen2.5-Math-1.5B						
Base	8.23	15.20	3.75	18.12	31.52	14.92
SFT	12.61	12.11	0.82	16.41	42.29	16.72
SFT (p)	25.19	27.38	7.72	38.12	65.79	32.94
Distill	25.46	23.64	6.68	37.50	60.92	30.83
TARGET-SFT	32.20	31.59	8.96	47.03	70.20	38.05
Qwen2.5-Math-7B						
Base	7.66	9.62	8.13	19.84	31.98	15.76
SFT	21.33	18.77	2.70	22.81	53.55	23.88
SFT (p)	28.48	32.78	8.56	49.38	67.93	37.33
Distill	23.35	18.79	5.63	30.31	51.24	25.76
TARGET-SFT	31.03	34.56	8.96	49.69	72.69	39.49
<i>Dataset: OpenR1-15k</i>						
Qwen3-1.7B-Base						
Base	9.87	11.35	0.62	16.25	33.81	14.26
SFT	14.30	12.55	1.65	20.62	41.68	18.31
SFT (p)	<u>25.86</u>	<u>23.66</u>	7.29	35.62	<u>62.41</u>	<u>31.23</u>
Distill	22.43	18.42	2.90	27.81	53.70	24.99
TARGET-SFT	27.47	24.78	<u>5.41</u>	<u>33.75</u>	63.92	31.41
Qwen2.5-Math-1.5B						
Base	8.23	15.20	3.75	18.12	31.52	14.92
SFT	14.45	15.35	1.87	24.22	43.99	19.71
SFT (p)	<u>31.18</u>	<u>33.56</u>	<u>11.45</u>	<u>47.34</u>	<u>70.75</u>	<u>39.00</u>
Distill	19.89	20.31	5.01	26.72	52.65	25.32
TARGET-SFT	33.09	34.84	13.13	51.72	72.38	41.24
Qwen2.5-Math-7B						
Base	7.66	9.62	8.13	19.84	31.98	15.76
SFT	34.41	33.26	11.88	50.16	73.29	40.55
SFT (p)	27.33	28.28	11.24	37.19	57.25	32.20
Distill	42.04	39.94	13.32	62.34	80.26	47.36
TARGET-SFT	43.61	42.42	18.13	<u>61.88</u>	80.75	49.50

in some cases, such as Qwen3-1.7B-Base (17.81 vs. 12.99) and Qwen2.5-Math-7B (25.76 vs. 23.88), whereas TARGET-SFT outperforms significantly. This suggests that simply replacing the target with a soft teacher distribution is still suboptimal. In contrast, TARGET-SFT uses the teacher to shape the residual branch, whose weight $1 - \gamma_t$ increases when y_t is under-supported. This adaptive use of teacher signals proves to be more effective than full distillation in these settings.

Medical. Table 2 shows a different pattern on medical reasoning. The gap between standard SFT and p -loss is smaller than in math, and in some cases standard SFT is clearly stronger. For example, on Qwen2.5-1.5B the two methods achieve similar averages, while on LLaMA-3.1-8B standard SFT substantially outperforms p -loss (47.41 vs. 38.60). This suggests that for some tasks, stricter imitation is more effective, perhaps because the demonstrations align more closely with the desired answer distribution. In such cases, the p -loss that uniformly weakens supervision for all low- p_y tokens is not ideal. Nevertheless, TARGET-SFT still achieves the best average performance across all models on the medical setting. This shows that the teacher-guided residual branch remains valuable even when probability-based reweighting alone is less effective. Distillation is also more competitive on medical reasoning than on math, outperforming p -loss on Qwen2.5-1.5B and Qwen2.5-7B. However,

Table 2: **Medical Reasoning.** Average@16 accuracy on medical reasoning benchmarks.

	MedMC	MedQA	PubMed	MMLU-P	GPQA	Lancet	MedB (4)	MedB (5)	MedX	NEJM	Avg.
LLaMA-3.2-3B											
Base	21.13	21.76	22.0	12.18	25.64	24.51	27.92	21.43	11.11	21.56	20.92
SFT	34.19	38.02	57.0	25.93	<u>30.26</u>	36.17	<u>36.04</u>	28.25	<u>11.73</u>	32.34	32.99
SFT (p)	40.43	<u>40.93</u>	<u>61.4</u>	33.42	34.87	<u>43.45</u>	34.09	25.97	9.87	40.30	<u>36.47</u>
Distill	37.08	38.26	55.7	28.01	27.44	39.81	35.71	31.82	10.01	35.16	33.90
TARGET-SFT	<u>39.78</u>	44.46	64.0	<u>32.70</u>	30.00	45.87	37.01	<u>31.17</u>	12.63	<u>39.30</u>	37.69
LLaMA-3.1-8B											
Base	22.81	29.30	21.2	19.02	29.49	22.82	29.87	20.78	10.14	20.07	22.55
SFT	50.47	<u>56.64</u>	<u>74.0</u>	<u>48.21</u>	<u>37.69</u>	<u>53.40</u>	47.73	40.26	14.77	50.91	<u>47.41</u>
SFT (p)	40.69	46.90	64.3	34.33	33.33	38.35	40.58	31.82	12.22	43.45	38.60
Distill	45.52	51.61	63.3	42.35	35.64	47.57	38.31	35.71	13.18	45.44	41.86
TARGET-SFT	<u>49.32</u>	60.17	74.7	50.42	46.15	55.34	<u>41.56</u>	<u>38.96</u>	<u>13.60</u>	<u>47.10</u>	47.73
Qwen2.5-1.5B											
Base	22.40	22.70	18.4	11.47	17.18	23.06	24.35	17.21	9.45	21.39	18.76
SFT	39.35	41.16	<u>68.5</u>	34.07	34.36	39.32	35.39	<u>30.19</u>	10.35	32.67	36.54
SFT (p)	38.92	37.55	67.6	37.79	35.64	<u>42.72</u>	35.71	<u>30.19</u>	10.49	36.48	37.31
Distill	41.02	42.58	68.9	<u>37.92</u>	<u>38.21</u>	43.20	<u>37.01</u>	28.57	<u>10.70</u>	38.97	<u>38.71</u>
TARGET-SFT	<u>40.31</u>	<u>41.87</u>	68.3	39.67	42.56	40.29	38.31	31.49	11.59	<u>38.64</u>	39.30
Qwen2.5-7B											
Base	51.35	57.03	69.7	54.01	<u>45.64</u>	56.80	42.21	40.26	12.22	<u>55.56</u>	48.48
SFT	42.24	44.07	69.3	41.43	36.67	42.96	38.64	37.01	12.01	39.30	40.36
SFT (p)	47.65	52.79	<u>74.5</u>	54.27	44.62	57.04	44.81	38.96	12.97	46.60	47.42
Distill	<u>52.28</u>	<u>58.84</u>	72.3	<u>58.89</u>	40.77	<u>58.01</u>	<u>50.65</u>	<u>41.56</u>	<u>13.73</u>	54.73	50.18
TARGET-SFT	54.53	62.37	74.9	60.85	48.21	59.95	52.92	42.86	14.01	56.55	52.72

TARGET-SFT still outperforms distillation across all models. The mixed performance of distillation again suggests that teacher information is useful, but treating it as a fixed full target is not always the best approach. Under the Q -target design, the teacher instead acts as adaptive fallback supervision, which supplements corrective signals for missing knowledge while preserving the model prior.

7.3 Ablation Study.

We ablate the two key design choices in TARGET-SFT. We include results on varying (1) *the intensity of teacher supervision* in the residual distribution, controlled by η . This tests the effect of the teacher model and the method’s sensitivity to this hyperparameter *etc.* We further vary (2) *the adaptive weighting of the residual branch*, controlled by $1 - \gamma_t$. This ablation directly tests whether using an uncertainty-dependent residual weight $1 - \gamma_t$ is effective, compared to simply assigning a fixed constant weight c to the $\tilde{\pi}_t$ branch. Additionally, we also tune the hyperparameter c for distillation to explore potential performance gain for the baseline.

We report the full results in Appendix E. In summary, the ablation studies validate both components of TARGET-SFT. While varying $\eta \in \{0.2, 0.5, 1.0\}$ gives averages in the range from 34.30 to 38.05, they all outperform the baselines and the best distillation setting (34.30 vs. 30.83). In contrast, further tuning of the hyperparameter $c \in \{0.2, 0.5, 0.8, 1.0\}$ for the distillation baseline does not lead to gains beyond the result presented in Table 1, but instead fluctuates significantly from 22.81 to 30.83. The ablation on residual weight $1 - \gamma_t$ also shows the effectiveness of this design, where changing to this to a constant c degrades the performance.

8 Conclusion

In this work, we show that supervised fine-tuning is fundamentally a target distribution design. We formalize this view through the Q -target framework $Q_t = \gamma_t \delta_{y_t} + (1 - \gamma_t) \tilde{\pi}_t$, which exposes two hidden design choices: how strongly to imitate the observed token, and how to allocate residual probability mass over alternatives. This lens unifies many existing SFT variants as implicit choices of γ_t or $\tilde{\pi}_t$. Building on this insight, we present TARGET-SFT and empirically demonstrate its effectiveness across ten reasoning data-model settings. Overall, our results offer a novel and more complete perspective into SFT, and open a broader design space for future SFT methods.

References

- [1] Shengyu Zhang, Linfeng Dong, Xiaoya Li, Sen Zhang, Xiaofei Sun, Shuhe Wang, Jiwei Li, Runyi Hu, Tianwei Zhang, Fei Wu, and Guoyin Wang. Instruction tuning for large language models: A survey, 2025.
- [2] Hyung Won Chung, Le Hou, Shayne Longpre, Barret Zoph, Yi Tay, William Fedus, Yunxuan Li, Xuezhi Wang, Mostafa Dehghani, Siddhartha Brahma, Albert Webson, Shixiang Shane Gu, Zhuyun Dai, Mirac Suzgun, Xinyun Chen, Aakanksha Chowdhery, Alex Castro-Ros, Marie Pellat, Kevin Robinson, Dasha Valter, Sharan Narang, Gaurav Mishra, Adams Yu, Vincent Zhao, Yanping Huang, Andrew Dai, Hongkun Yu, Slav Petrov, Ed H. Chi, Jeff Dean, Jacob Devlin, Adam Roberts, Denny Zhou, Quoc V. Le, and Jason Wei. Scaling instruction-finetuned language models, 2022.
- [3] Long Ouyang, Jeff Wu, Xu Jiang, Diogo Almeida, Carroll L. Wainwright, Pamela Mishkin, Chong Zhang, Sandhini Agarwal, Katarina Slama, Alex Ray, John Schulman, Jacob Hilton, Fraser Kelton, Luke Miller, Maddie Simens, Amanda Askell, Peter Welinder, Paul Christiano, Jan Leike, and Ryan Lowe. Training language models to follow instructions with human feedback, 2022.
- [4] Arnav Gudibande, Eric Wallace, Charlie Snell, Xinyang Geng, Hao Liu, Pieter Abbeel, Sergey Levine, and Dawn Song. The false promise of imitating proprietary llms, 2023.
- [5] Ziniu Li, Congliang Chen, Tian Xu, Zeyu Qin, Jiancong Xiao, Zhi-Quan Luo, and Ruoyu Sun. Preserving diversity in supervised fine-tuning of large language models, 2025.
- [6] Gaotang Li, Ruizhong Qiu, Xiusi Chen, Heng Ji, and Hanghang Tong. Beyond log likelihood: Probability-based objectives for supervised fine-tuning across the model capability continuum, 2026.
- [7] Bolin Zhang, Jiahao Wang, Qianlong Du, Jiajun Zhang, Zhiying Tu, and Dianhui Chu. A survey on data selection for llm instruction tuning. *Journal of Artificial Intelligence Research*, 83, August 2025.
- [8] Alon Albalak, Yanai Elazar, Sang Michael Xie, Shayne Longpre, Nathan Lambert, Xinyi Wang, Niklas Muennighoff, Bairu Hou, Liangming Pan, Haewon Jeong, Colin Raffel, Shiyu Chang, Tatsunori Hashimoto, and William Yang Wang. A survey on data selection for language models, 2024.
- [9] Zheng Yuan, Hongyi Yuan, Chengpeng Li, Guanting Dong, Keming Lu, Chuanqi Tan, Chang Zhou, and Jingren Zhou. Scaling relationship on learning mathematical reasoning with large language models, 2023.
- [10] Chunting Zhou, Pengfei Liu, Puxin Xu, Srini Iyer, Jiao Sun, Yuning Mao, Xuezhe Ma, Avia Efrat, Ping Yu, Lili Yu, Susan Zhang, Gargi Ghosh, Mike Lewis, Luke Zettlemoyer, and Omer Levy. Lima: Less is more for alignment, 2023.
- [11] Tao Liu, Taiqiang Wu, Runming Yang, Shaoning Sun, Junjie Wang, and Yujiu Yang. Profit: Leveraging high-value signals in sft via probability-guided token selection, 2026.
- [12] Shenzhi Wang, Le Yu, Chang Gao, Chujie Zheng, Shixuan Liu, Rui Lu, Kai Dang, Xionghui Chen, Jianxin Yang, Zhenru Zhang, Yuqiong Liu, An Yang, Andrew Zhao, Yang Yue, Shiji Song, Bowen Yu, Gao Huang, and Junyang Lin. Beyond the 80/20 rule: High-entropy minority tokens drive effective reinforcement learning for llm reasoning, 2025.
- [13] Yongliang Wu, Yizhou Zhou, Zhou Ziheng, Yingzhe Peng, Xinyu Ye, Xinting Hu, Wenbo Zhu, Lu Qi, Ming-Hsuan Yang, and Xu Yang. On the generalization of sft: A reinforcement learning perspective with reward rectification, 2026.
- [14] Tianzhe Chu, Yuexiang Zhai, Jihan Yang, Shengbang Tong, Saining Xie, Dale Schuurmans, Quoc V. Le, Sergey Levine, and Yi Ma. Sft memorizes, rl generalizes: A comparative study of foundation model post-training, 2025.

- [15] Idan Shenfeld, Jyothish Pari, and Pulkit Agrawal. RI’s razor: Why online reinforcement learning forgets less, 2025.
- [16] Howard Chen, Noam Razin, Karthik Narasimhan, and Danqi Chen. Retaining by doing: The role of on-policy data in mitigating forgetting, 2025.
- [17] Jerry Huang, Peng Lu, and Qiu hao Zeng. Calibrated language models and how to find them with label smoothing, 2025.
- [18] Dylan Zhang, Qirun Dai, and Hao Peng. The best instruction-tuning data are those that fit, 2026.
- [19] Zhiwen Ruan, Yixia Li, He Zhu, Yun Chen, Peng Li, Yang Liu, and Guanhua Chen. Enhancing large language model reasoning via selective critical token fine-tuning, 2025.
- [20] Muxi Diao, Lele Yang, Wuxuan Gong, Yutong Zhang, Zhonghao Yan, Yufei Han, Kongming Liang, Weiran Xu, and Zhanyu Ma. Entropy-adaptive fine-tuning: Resolving confident conflicts to mitigate forgetting, 2026.
- [21] He Zhu, Junyou Su, Peng Lai, Ren Ma, Wenjia Zhang, Linyi Yang, and Guanhua Chen. Anchored supervised fine-tuning, 2026.
- [22] Wenhong Zhu, Ruobing Xie, Rui Wang, Xingwu Sun, Di Wang, and Pengfei Liu. Proximal supervised fine-tuning, 2026.
- [23] Chongli Qin and Jost Tobias Springenberg. Supervised fine tuning on curated data is reinforcement learning (and can be improved), 2025.
- [24] Longhui Yu, Weisen Jiang, Han Shi, Jincheng Yu, Zhengying Liu, Yu Zhang, James T. Kwok, Zhenguo Li, Adrian Weller, and Weiyang Liu. Metamath: Bootstrap your own mathematical questions for large language models, 2024.
- [25] Lichang Chen, Shiyang Li, Jun Yan, Hai Wang, Kalpa Gunaratna, Vikas Yadav, Zheng Tang, Vijay Srinivasan, Tianyi Zhou, Heng Huang, and Hongxia Jin. Alpapasus: Training a better alpaca with fewer data, 2024.
- [26] Avi Singh, John D. Co-Reyes, Rishabh Agarwal, Ankesh Anand, Piyush Patil, Xavier Garcia, Peter J. Liu, James Harrison, Jaehoon Lee, Kelvin Xu, Aaron Parisi, Abhishek Kumar, Alex Alemi, Alex Rizkowsky, Azade Nova, Ben Adlam, Bernd Bohnet, Gamaleldin Elsayed, Hanie Sedghi, Igor Mordatch, Isabelle Simpson, Izzeddin Gur, Jasper Snoek, Jeffrey Pennington, Jiri Hron, Kathleen Kenealy, Kevin Swersky, Kshiteej Mahajan, Laura Culp, Lechao Xiao, Maxwell L. Bileschi, Noah Constant, Roman Novak, Rosanne Liu, Tris Warkentin, Yundi Qian, Yamini Bansal, Ethan Dyer, Behnam Neyshabur, Jascha Sohl-Dickstein, and Noah Fiedel. Beyond human data: Scaling self-training for problem-solving with language models, 2024.
- [27] Zixiang Chen, Yihe Deng, Huizhuo Yuan, Kaixuan Ji, and Quanquan Gu. Self-play fine-tuning converts weak language models to strong language models, 2024.
- [28] Eric Zelikman, Yuhuai Wu, Jesse Mu, and Noah D. Goodman. Star: Bootstrapping reasoning with reasoning, 2022.
- [29] Wei Xiong, Jiarui Yao, Yuhui Xu, Bo Pang, Lei Wang, Doyen Sahoo, Junnan Li, Nan Jiang, Tong Zhang, Caiming Xiong, and Hanze Dong. A minimalist approach to llm reasoning: from rejection sampling to reinforce, 2025.
- [30] Zhaorui Yang, Tianyu Pang, Haozhe Feng, Han Wang, Wei Chen, Minfeng Zhu, and Qian Liu. Self-distillation bridges distribution gap in language model fine-tuning, 2024.
- [31] Yuxian Gu, Li Dong, Furu Wei, and Minlie Huang. Minillm: On-policy distillation of large language models, 2026.
- [32] Jia LI, Edward Beeching, Lewis Tunstall, Ben Lipkin, Roman Soletskyi, Shengyi Costa Huang, Kashif Rasul, Longhui Yu, Albert Jiang, Ziju Shen, Zihan Qin, Bin Dong, Li Zhou, Yann Fleureau, Guillaume Lample, and Stanislas Polu. Numinamath. [<https://huggingface.co/AI-MO/NuminaMath-CoT>] (https://github.com/project-numina/aimo-progress-prize/blob/main/report/numina_dataset.pdf), 2024.

- [33] Elie Bakouch, Leandro von Werra, and Lewis Tunstall. Open-r1: a fully open reproduction of deepseek-r1. <https://huggingface.co/blog/open-r1>, January 2025. Hugging Face Blog.
- [34] Jianhao Yan, Yafu Li, Zican Hu, Zhi Wang, Ganqu Cui, Xiaoye Qu, Yu Cheng, and Yue Zhang. Learning to reason under off-policy guidance, 2025.
- [35] Xiaoke Huang, Juncheng Wu, Hui Liu, Xianfeng Tang, and Yuyin Zhou. m1: Unleash the potential of test-time scaling for medical reasoning with large language models, 2026.
- [36] Geoffrey Hinton, Oriol Vinyals, and Jeff Dean. Distilling the knowledge in a neural network, 2015.
- [37] Aitor Lewkowycz, Anders Andreassen, David Dohan, Ethan Dyer, Henryk Michalewski, Vinay Ramasesh, Ambrose Slone, Cem Anil, Imanol Schlag, Theo Gutman-Solo, Yuhuai Wu, Behnam Neyshabur, Guy Gur-Ari, and Vedant Misra. Solving quantitative reasoning problems with language models, 2022.
- [38] XTX Investments. Ai mathematical olympiad - progress prize 1. <https://kaggle.com/competitions/ai-mathematical-olympiad-prize>, 2024. Kaggle.
- [39] Mathematical Association of America. Aime thresholds are available. <https://maa.org/aime-thresholds-are-available/>, 2024. Accessed: 2025-09-24.
- [40] Mathematical Association of America. Math competitions. <https://maa.org/math-competitions>, 2023. Accessed: 2025-09-24.
- [41] Dan Hendrycks, Collin Burns, Saurav Kadavath, Akul Arora, Steven Basart, Eric Tang, Dawn Song, and Jacob Steinhardt. Measuring mathematical problem solving with the math dataset, 2021.
- [42] Ankit Pal, Logesh Kumar Umapathi, and Malaikannan Sankarasubbu. Medmcqa : A large-scale multi-subject multi-choice dataset for medical domain question answering, 2022.
- [43] Di Jin, Eileen Pan, Nassim Oufattole, Wei-Hung Weng, Hanyi Fang, and Peter Szolovits. What disease does this patient have? a large-scale open domain question answering dataset from medical exams, 2020.
- [44] Qiao Jin, Bhuwan Dhingra, Zhengping Liu, William W. Cohen, and Xinghua Lu. Pubmedqa: A dataset for biomedical research question answering, 2019.
- [45] Yubo Wang, Xueguang Ma, Ge Zhang, Yuansheng Ni, Abhranil Chandra, Shiguang Guo, Weiming Ren, Aaran Arulraj, Xuan He, Ziyang Jiang, Tianle Li, Max Ku, Kai Wang, Alex Zhuang, Rongqi Fan, Xiang Yue, and Wenhua Chen. Mmlu-pro: A more robust and challenging multi-task language understanding benchmark, 2024.
- [46] David Rein, Betty Li Hou, Asa Cooper Stickland, Jackson Petty, Richard Yuanzhe Pang, Julien Dirani, Julian Michael, and Samuel R. Bowman. Gpqa: A graduate-level google-proof q&a benchmark, 2023.
- [47] Hanjie Chen, Zhouxiang Fang, Yash Singla, and Mark Dredze. Benchmarking large language models on answering and explaining challenging medical questions, 2026.
- [48] Yuxin Zuo, Shang Qu, Yifei Li, Zhangren Chen, Xuekai Zhu, Ermo Hua, Kaiyan Zhang, Ning Ding, and Bowen Zhou. Medxpertqa: Benchmarking expert-level medical reasoning and understanding, 2025.

A Experiment Details

Training Configurations. All SFT experiments are conducted using `ver1`, largely following the work by Li et al. [6]. The optimizer used is AdamW, with the learning rate of 5×10^{-5} for all models. We use cosine decay scheduling with a warm-up ratio of 0.1. We use the maximum sequence length of 3072 for both mathematical reasoning datasets. The global train batch size is 256, with gradient accumulation. The experiments are conducted on A6000 and H200 GPUs. All models are trained for 1 epoch. Table 3 summarizes all training and evaluation-related configurations.

Teacher Models. For methods that involve teacher distribution, we use the corresponding instruction-tuned model as the teacher for the base model; for example, Qwen2.5-1.5B uses Qwen2.5-1.5B-Instruct. For Qwen3-1.7B-Base, we use Qwen3-4B-Instruct-2507 as the teacher. For TARGET-SFT, we choose the teacher signal intensity from $\eta \in \{0.2, 0.5, 1.0\}$. To ensure consistency across methods, we cache all teacher logits before training and use the same cache for both distillation and TARGET-SFT experiments. For memory efficiency, the cached teacher distribution is truncated to the top-64 tokens in the vocabulary with the highest probabilities.

Datasets. For NuminaMath-CoT which originally contains 859k chain-of-through problems, we following Li et al. [6] and use the 67k subset organized in their work. For the OpenR1 training dataset, we sample 15k from OpenR1-Math-46k-8192 [34], which contains verified traces generated by DeepSeek-R1 for problems collected from NuminaMath 1.5 [32]. We collect the responses with sequence length shorter than 3072 to standardize with the training configuration for NuminaMath-CoT. For scientific reasoning, we use m23k [35], a 23k high-quality medical reasoning dataset.

Evaluation. For mathematical reasoning, evaluation covers five representative benchmarks: Minerva Math, Olympiad Bench, AIME24, AMC23, and Math500 [37, 38, 39, 40, 41]. For models trained on m23k, we evaluate on the same benchmarks following Li et al. [6], which include MedMCQA [42], MedQA-USMLE [43], PubMedQA [44], MMLU-Pro [45], GPQA (Medical) [46], Lancet & NEJM [35], MedBullets [47], and MedXpertQA [48]. Evaluation follows the same protocol as Li et al. [6] and Huang et al [35]. Inference uses a maximum generation length of 4096 tokens with the decoding temperature 1.0. For distillation and TARGET-SFT on Qwen2.5-Math-7B trained from the longer-sequence OpenR1-15k dataset, we use the decoding settings with temperature 0.7 and top-p 0.8 as recommended for its teacher model Qwen2.5-Math-7B-Instruct. The reported results are averaged over 16 generations for every prompt.

Table 3: **Configuration summary.** All experiments use the same setup unless otherwise specified.

Section	Item	Details
Dataset	NuminaMath-CoT	67k subset from Li et al. [6]
	OpenR1	15k samples with length < 3072 from OpenR1-Math-46k-8192 [34]
	Medical reasoning	m23k [35], a 23k high-quality medical reasoning dataset
Model	Math	Qwen3-1.7B-Base, Qwen2.5-Math-1.5B, Qwen2.5-Math-7B
	Medical	LLaMA-3.2-3B, LLaMA-3.1-8B, Qwen2.5-1.5B, Qwen2.5-7B
Train	Framework	<code>ver1</code>
	Optimizer	AdamW
	Learning rate	5×10^{-5}
	Schedule	Cosine decay with warm-up ratio 0.1
	Max sequence length	3072
	Global batch size	256, with gradient accumulation
	Epochs	1
Eval	Max generation length	4096
	Metric	Average@16

B Proofs

B.1 Proof of Proposition 1

For a target distribution Q_t , the token-level cross-entropy loss is

$$\text{CE}(Q_t, \pi_\theta(\cdot | x_t)) = - \sum_{k \in \mathcal{V}} Q_t(k) \log \pi_\theta(k | x_t).$$

By definition, the Q-target is

$$Q_t = \gamma_t \delta_{y_t} + (1 - \gamma_t) \tilde{\pi}_t.$$

Substituting this into the cross-entropy gives

$$\begin{aligned} \text{CE}(Q_t, \pi_\theta(\cdot | x_t)) &= - \sum_{k \in \mathcal{V}} [\gamma_t \delta_{y_t}(k) + (1 - \gamma_t) \tilde{\pi}_t(k)] \log \pi_\theta(k | x_t) \\ &= -\gamma_t \sum_{k \in \mathcal{V}} \delta_{y_t}(k) \log \pi_\theta(k | x_t) - (1 - \gamma_t) \sum_{k \in \mathcal{V}} \tilde{\pi}_t(k) \log \pi_\theta(k | x_t) \\ &= \gamma_t \text{CE}(\delta_{y_t}, \pi_\theta(\cdot | x_t)) + (1 - \gamma_t) \text{CE}(\tilde{\pi}_t, \pi_\theta(\cdot | x_t)). \end{aligned} \quad (9)$$

Therefore, training toward Q_t decomposes the token-level supervision into two components: label imitation controlled by γ_t and residual distribution matching of $\tilde{\pi}_t$.

B.2 Proof of Corollary 1

Given the token-weighted loss with detached importance weighting w_t

$$\mathcal{L}_t^w = -w_t \log \pi_\theta(y_t | x_t),$$

we consider the choice of $(\gamma_t, \tilde{\pi}_t)$

$$(\gamma_t = w_t, \tilde{\pi}_t = \text{sg}[\pi_\theta(\cdot | x_t)]) \implies Q_t = w_t \delta_{y_t} + (1 - w_t) \text{sg}[\pi_\theta(\cdot | x_t)].$$

By Proposition 1, the token-level loss for this Q_t decomposes as

$$\text{CE}(Q_t, \pi_\theta) = w_t \text{CE}(\delta_{y_t}, \pi_\theta) + (1 - w_t) \text{CE}(\text{sg}[\pi_\theta], \pi_\theta).$$

The first term gives the token-weighted SFT gradient:

$$\nabla_\theta w_t \text{CE}(\delta_{y_t}, \pi_\theta) = -w_t \nabla_\theta \log \pi_\theta(y_t | x_t).$$

For the second term, let $p_t = \pi_\theta$ and $\bar{p}_t = \text{sg}[p_t]$. Since the logit gradient of $\text{CE}(\bar{p}_t, p_t)$ is $p_t - \bar{p}_t$, and \bar{p}_t is a detached copy of p_t , we have

$$\nabla_\theta \text{CE}(\text{sg}[p_t], p_t) = 0.$$

Therefore,

$$\nabla_\theta \text{CE}(Q_t, \pi_\theta) = -w_t \nabla_\theta \log \pi_\theta(y_t | x_t) = \nabla_\theta \mathcal{L}_t^w. \quad (10)$$

This shows that token-weighted SFT is equivalent at the gradient level to Q-target training with $\gamma_t = w_t$ and a self-matching residual branch $\tilde{\pi}_t = \text{sg}[\pi_\theta]$.

B.3 Proof of Corollary 2

Given the distributional objective

$$\mathcal{L}_t = -a_t \log \pi_\theta(y_t | x_t) + b_t \text{CE}(q_t, \pi_\theta), \quad a_t, b_t \geq 0,$$

rewrite the label imitation term as cross-entropy and obtain:

$$\mathcal{L}_t = a_t \text{CE}(\delta_{y_t}, \pi_\theta) + b_t \text{CE}(q_t, \pi_\theta).$$

Let $s_t = a_t + b_t$. For $s_t > 0$, this can be normalized as

$$\mathcal{L}_t = s_t \left[\frac{a_t}{s_t} \text{CE}(\delta_{y_t}, \pi_\theta) + \frac{b_t}{s_t} \text{CE}(q_t, \pi_\theta) \right].$$

The constant s_t only rescales the token-level gradient globally, which can be absorbed into the effective learning rate or token weight. Define

$$\gamma_t = \frac{a_t}{a_t + b_t}, \quad \tilde{\pi}_t = q_t.$$

By linearity of cross-entropy in its first argument,

$$\gamma_t \text{CE}(\delta_{y_t}, \pi_\theta) + (1 - \gamma_t) \text{CE}(\tilde{\pi}_t, \pi_\theta) = \text{CE}(\gamma_t \delta_{y_t} + (1 - \gamma_t) \tilde{\pi}_t, \pi_\theta). \quad (11)$$

Therefore, up to the overall scale $a_t + b_t$, the objective is equivalent to Q-target training with

$$Q_t = \gamma_t \delta_{y_t} + (1 - \gamma_t) \tilde{\pi}_t.$$

This proves the claim of Corollary 2.

Some distributional methods fall outside the nonnegative residual-mixture form in Eq. (4). For example, GEM [5] discourages model from concentrating high probability on the strongest non-label alternatives. This can be expressed schematically as a repulsive branch $\tilde{\pi}_{t,\tau}^-$ as follows

$$\tilde{\pi}_{t,\tau}^-(k) = \frac{\pi_\theta(k | x_t)^{1/\tau}}{\sum_{v \in \mathcal{V}} \pi_\theta(v | x_t)^{1/\tau}}, \quad \tau < 1.$$

This represents a τ -sharpened model distribution, which places mass on high-probability tokens. And its objective is conceptually written as

$$\mathcal{L}_t = \text{CE}(\delta_{y_t}, \pi_\theta) - \lambda \text{CE}(\tilde{\pi}_{t,\tau}^-, \pi_\theta),$$

shaping the residual branch repulsively against collapsing onto a small set of tokens, thereby aligning with GEM’s goal of preserving diversity in SFT.

This can be viewed as a signed residual extension of the Q-target framework, with $\tilde{\pi}_t = (\tilde{\pi}_t^+, \tilde{\pi}_t^-)$. This defines a *desired and undesired* target alternative, where $Q_t = \delta_{y_t} + \tilde{\pi}_t^+ + \tilde{\pi}_t^-$. Instead of matching a positive residual distribution, GEM specifies an undesired residual direction to preserve diversity. More generally under this view, distributional variants can shape the residual branch to emphasize or suppress particular subsets of tokens.

C Unifying Framework

In this section, we provide concrete connections between SFT variants discussed in Section 2 and our Q -target perspective. Table 4 shows the loss formulation and core motivation for each variant. Following the formulation $Q_t = \gamma_t \delta_{y_t} + (1 - \gamma_t) \tilde{\pi}_t$, these methods can be interpreted through their choices of γ_t and $\tilde{\pi}_t$, as summarized in Table 5.

Table 4: **Details of SFT Variants.** Each method is presented as a token-level objective ℓ_t , given the prefix x_t and observed token y_t . We denote $p_t = \pi_\theta(y_t | x_t)$, $p_\theta(v) = \pi_\theta(v | x_t)$, $\text{sg}[\cdot]$ as stop-gradient, π_T, π_S as teacher and student distribution, and \mathcal{V} as the vocabulary.

SFT Variant	Token-level Objective	Motivation
Standard SFT	$\ell_t^{\text{SFT}} = -\log p_t$	Maximize likelihood of every observed token
<i>Token-Level Variants</i>		
DFT [13]	$\ell_t^{\text{DFT}} = -\text{sg}[p_t] \log p_t$	Use weighting to connect SFT with an RL-style objective
Beyond-log [6]	$\ell_t^f = f(p_t), \quad \ell_t^\alpha = \frac{1 - p_t^\alpha}{\alpha}$	Use probability-dependent objectives to balance learning across model capacities
ProFiT [11]	$m_t = \mathbf{1}[\text{sg}(p_t) > \tau],$ $\ell_t^{\text{ProFiT}} = -m_t \log p_t$	Use probability to identify and train on core tokens
EAFt [20]	$\tilde{H}_t = \text{sg} \left[\frac{H(\pi_{\theta,t}^{(k)})}{\log k} \right],$ $\ell_t^{\text{EAFt}} = -\tilde{H}_t \log p_t.$	Use entropy to weight uncertain or knowledge-conflicting tokens
iw-SFT [23]	$w(\tau) = \frac{q(\tau)}{\pi_{\text{ref}}(\tau)},$ (w trajectory-level) $\ell_t^{\text{iw}} = -w(\tau) \log p_t$	Use an auxiliary distribution to assign trajectory-level weights
CFT [19]	$c_t = \mathbf{1}[\forall \tilde{y}_t \in \mathcal{A}_t, \text{Correct}(y_{<t}, \tilde{y}_t, y_{>t}) = 0],$ $\ell_t^{\text{CFT}} = -c_t \log p_t$	Update only causally critical / irreplaceable tokens
<i>Distributional-Level Variants</i>		
Label Smooth [17]	$\ell_t^{\text{LS}} = -[(1 - \lambda) \log p_t + \frac{\lambda}{ \mathcal{V} } \sum_{v \in \mathcal{V}} \log p_{\theta,t}(v)]$	Regularize overconfident predictions for better calibration
SFT + KL [15]	$\ell_t^{\text{KL}} = -\log p_t + \lambda \text{KL}(\pi_{\text{ref}}(\cdot x_t) \ \pi_\theta(\cdot x_t))$	Constrain updates with a reference model to limit drift
ASFT [21]	$\ell_t^{\text{ASFT}} = \ell_t^{\text{DFT}} + \lambda \text{KL}(\pi_{\text{base}}(\cdot x_t) \ \pi_\theta(\cdot x_t))$	Constrain updates in DFT to prevent distributional drift
Proximal SFT [22]	$r_t = \frac{p_t}{\pi_{\text{old}}(y_t x_t)},$ $\ell_t^{\text{PSFT}} = -\min(r_t, \text{clip}(r_t, 1 - \epsilon, 1 + \epsilon))$	Clip ratio to enforce updates within a trust region
GEM [5]	$q_t(v) = \frac{\text{sg}[\pi_{\theta,t}(v)]^{1/\beta}}{\sum_{u \in \mathcal{V}} \text{sg}[\pi_{\theta,t}(u)]^{1/\beta}},$ $\ell_t^{\text{GEM}} = \text{CE}(\delta_{y_t}, \pi_{\theta,t}) - \text{CE}(q_t, \pi_{\theta,t})$	Control probability transfer from alternatives to observed token to preserve diversity
Knowledge Distillation [36]	$\ell_t^{\text{KD}} = -\sum_{v \in \mathcal{V}} \pi_T(v x_t) \log \pi_S(v x_t)$	Use the teacher logit distribution as a soft target
Distillation (Hybrid) [36]	$\ell_t^{\text{KD-H}} = (1 - \lambda)[- \log \pi_S(y_t x_t)]$ $+ \lambda D_{\text{KL}}(\pi_T(\cdot x_t) \ \pi_S(\cdot x_t))$	Use hard-label and enrich it with teacher logit distribution

We organize existing methods into three broad categories. **Label-trust** variants modify the imitation strength on y_t , corresponding to different choices of γ_t . **Residual-distribution** variants primarily specify where the non-label probability mass should go. In these cases, the corresponding γ_t is often obtained by normalizing the relative weights of the hard-label and residual branches, with any overall scale absorbed into the effective learning rate. Finally, **data-level** methods do not directly alter γ_t or $\tilde{\pi}_t$ for a fixed demonstration. Instead, they reshape the empirical target distribution by selecting, filtering, or rewriting the training trajectory \hat{y} , after which standard one-hot SFT is applied. We therefore include them as indirect instances of target distribution design at the dataset level.

In particular, GEM [5] can also be illustrated with a signed extension of the Q -framework, where the residual component contains both positive and negative branches, $\tilde{\pi}_t = (\tilde{\pi}_t^+, \tilde{\pi}_t^-)$. This defines a *desired and undesired* target alternative, where $Q_t = \delta_{y_t} + \tilde{\pi}_t^+ + \tilde{\pi}_t^-$. And GEM utilizes $\tilde{\pi}_t^-$ as a repulsive branch to discourage probability collapse onto a small set of high-probability tokens, hence preserving diversity. Proximal SFT [22] is included as a schematic connection, since its clipping-based trust-region objective is not an explicit residual target but implicitly constrains updates.

Throughout the table, $(\gamma_t, \tilde{\pi}_t)$ are treated as stop-gradient unless otherwise specified. Some methods are originally defined at the sequence or trajectory level [23, 19], we present their token-level decompositions or analogues to make the connection to Q_t explicit.

Table 5: **SFT variants under the Q -target view.** Each method can be interpreted through choices of label trust γ_t and residual distribution $\tilde{\pi}_t$ in $Q_t = \gamma_t \delta_{y_t} + (1 - \gamma_t) \tilde{\pi}_t$. This table provides illustrative examples rather than an exhaustive coverage of methods in each category.

Variant	Category	Choice of γ_t	Choice of $\tilde{\pi}_t$
Standard SFT	One-hot imitation	1	–
DFT [13]	Label Trust	p_t	$\pi_{\theta,t}$
Beyond-log [6]	Label Trust	p_t^α	$\pi_{\theta,t}$
ProFiT [11]	Label Trust	$m_t = \mathbf{1}\{p_t > \tau\}$	$\pi_{\theta,t}$
EAFT [20]	Label Trust	$\tilde{H}_t = \frac{H(\pi_{\theta,t}^{(k)})}{\log k}$	$\pi_{\theta,t}$
iw-SFT [23]	Label Trust	$w(\tau) = \frac{q(\tau)}{\pi_{\text{ref}}(\tau)}$, (trajectory-level)	$\pi_{\theta,t}$
CFT [19]	Label Trust	$c_t = \mathbf{1}\{y_t \text{ counterfactual critical}\}$	$\pi_{\theta,t}$
Label Smoothing [17]	Residual Distribution	$1 - \lambda$	$\text{Unif}(\mathcal{V})$
SFT + KL [15]	Residual Distribution	$\frac{1}{1+\lambda}$	$\pi_{\text{ref}}(\cdot x_t)$
ASFT [21]	Residual Distribution	$\frac{p_t}{p_t + \lambda}$	$\pi_{\text{base}}(\cdot x_t)$
Proximal SFT [22]	Residual Distribution	clipping-dependent	$\pi_{\text{old}}(\cdot x_t)$
GEM [5]	Residual Distribution	$\gamma_t^y = 1, \gamma_t^- = 1$	$\tilde{\pi}_t^+ = \pi_{\theta,t}, \tilde{\pi}_t^- = \pi_{\theta,t}^{(\beta)}$
Knowledge Distillation [36]	Residual Distribution	0	$\pi_T(\cdot x_t)$
Distillation (Hybrid) [36]	Residual Distribution	$1 - \lambda$	$\pi_T(\cdot x_t)$
RFT [9]	Data-Level	–	$\delta_{\hat{y}}, \hat{y} \sim \pi_{\text{gen, correct}}(\cdot x)$
STaR [28]	Data-Level	–	$\delta_{\hat{y}}, \hat{y} \sim \pi_{\text{gen, correct}}(\cdot x)$
GRAPE [18]	Data-Level	–	$\delta_{\hat{y}}, \hat{y} = \arg \max_{y^{(i)}} \pi_{\theta_0}(y^{(i)} x)$
Self-distillation [30]	Data-Level	–	$\delta_{\hat{y}}, \hat{y} = \text{Rewrite}_{\pi_{\theta_0}}(x, y)$
TARGET-SFT	Label Trust + Residual	p_t	$\tilde{\pi}_t^{\text{guided}} \propto \pi_{\theta,t}^{1-\eta} \pi_T(\cdot x_t)^\eta$

D From Any Loss to Q_t

Section 5.2 introduces the derivation of Q -target from any differentiable token-level SFT loss. We now provide two examples and visualize their effects below.

Example 1: Standard SFT. Standard SFT minimizes the negative log-likelihood of the observed token $\mathcal{L}_{\text{SFT}}(z) = -\log p_y$, where p_y is the model probability assigned to y . The logit gradient is

$$g_j = \frac{\partial \mathcal{L}_{\text{SFT}}}{\partial z_j} = p_j - \mathbf{1}\{j = y\}. \quad (12)$$

Substituting this into Eq. (6), we obtain the induced target

$$Q_{\text{SFT}}(j) = p_j - g_j = \begin{cases} 1, & j = y, \\ 0, & j \neq y. \end{cases} \quad (13)$$

This recovers exactly the one-hot target distribution δ_y , assigning all target mass to the observed token and zero mass to alternatives.

Example 2: Probability-Weighted SFT. Consider the detached probability-weighted loss

$$\mathcal{L}_{p\text{-loss}}(z) = -\text{sg}[p_y] \log p_y, \quad (14)$$

This loss has the logit gradient

$$g_j = \text{sg}[p_y](p_j - \mathbf{1}\{j = y\}). \quad (15)$$

Substituting this gradient into Eq. (6), and using the scalar $\text{sg}[p_y] = p_y$ derives the induced target

$$Q_{p\text{-loss}}(j) = \begin{cases} 2p_y - p_y^2, & j = y, \\ (1 - p_y)p_j, & j \neq y. \end{cases} \quad (16)$$

This closed form reveals the mechanism of probability-weighted SFT. When the model assigns high probability to the observed token ($p_y \rightarrow 1$), the induced target approaches the one-hot SFT target. When the model is uncertain ($p_y \rightarrow 0$), the induced target relaxes toward the model’s own distribution $Q_j \rightarrow p_j$. Thus, low-confidence tokens receive weaker imitation updates, and the residual probability mass defaults to the student prior. In the Q -target notation, this corresponds to choosing $\gamma = p_y$ and $\tilde{\pi} = \text{sg}[\pi_\theta]$, thereby preserving the model prior when evidence for strict imitation on y is weak.

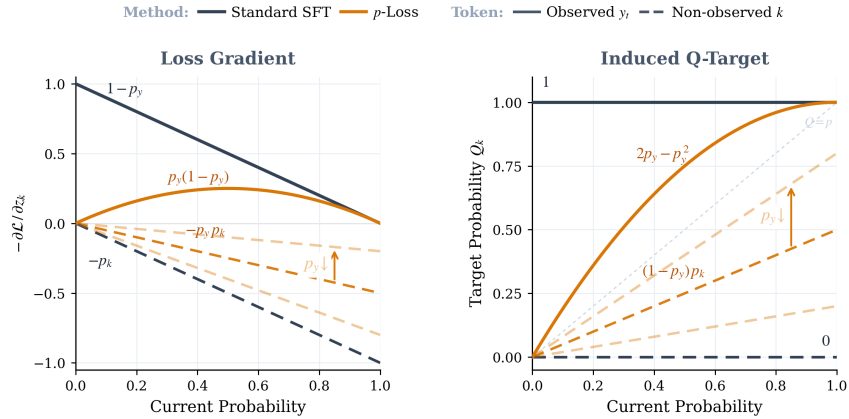


Figure 3: **Visualization of Loss.** Standard SFT’s gradient pulls toward y_t and suppresses all k with fixed strength, corresponding to an induced target δ_{y_t} . For p -loss, the gradient scales with p_y (slope for Non-observed token k depends on p_y). Therefore, its gradient is near-zero when $p_y \approx 0$, and the target probability is the same as current probability ($Q = p$); the induced target approaches δ_{y_t} only when $p_y \rightarrow 1$, where the model is certain. An interactive plot is available on our [project page](#).

E Ablation Study

We ablate on the two key design choices in TARGET-SFT: (1) **intensity of teacher supervision** in the residual distribution, controlled by η , and (2) **adaptive weighting of the residual branch**, controlled by $1 - \gamma_t$. The first ablation tests the effect of teacher model and the method’s sensitivity to this hyperparameter η . The second ablation tests whether using an uncertainty-dependent residual weight $1 - \gamma_t$ is useful, compared to simply assigning a fixed constant weight c to the $\tilde{\pi}_t$ branch.

Additionally, we ablate on the hyperparameter $c = \{0.2, 0.5, 0.8, 1.0\}$ in the knowledge distillation baseline ($\mathcal{L}_{\text{Distill}} = c \text{CE}(\pi_T, \pi_\theta) + (1 - c) \text{CE}(\delta_{y_t}, \pi_\theta)$). This presents further results on baseline performance beyond the default choice of $c = 0.8$ used in the main text.

Table 6: **Ablation Study.** Average@16 accuracy using Qwen2.5-Math-1.5B trained on NuminaMath (top) and OpenR1 (bottom) to ablate on two key designs of the method.

	Minerva Math	Olympiad Bench	AIME24	AMC23	Math500	Avg.
<i>Intensity of teacher signal η ($\eta \uparrow =$ dominant supervision)</i>						
Distill ($c = 0.2$)	13.99	13.08	1.45	17.34	44.32	18.33
Distill ($c = 0.5$)	19.13	18.94	4.16	26.56	53.81	24.92
Distill ($c = 0.8$)	25.46	23.64	6.68	37.50	60.92	30.83
Distill ($c = 1.0$)	18.07	18.49	4.38	28.28	45.22	22.81
TARGET-SFT ($\eta = 0.2$)	27.41	29.48	9.17	44.06	65.96	35.16
TARGET-SFT ($\eta = 0.5$)	32.20	31.59	8.96	47.03	70.20	38.05
TARGET-SFT ($\eta = 1.0$)	28.24	28.13	7.92	43.12	63.85	34.30
<i>Constant branch c, instead of residual $1 - \gamma_t$</i>						
$c = 0.2$	22.09	23.23	5.00	33.44	58.24	28.48
$c = 0.5$	29.54	33.19	11.67	50.47	70.71	39.10
$c = 1.0$	22.27	27.26	8.14	41.72	60.32	31.82
TARGET-SFT	33.09	34.84	13.13	51.72	72.38	41.24

The results in Table 6 show that TARGET-SFT still achieves the highest results among all baselines. On the other hand, knowledge distillation in this setting is highly sensitive to the mixture weight c . In particular, it requires intricate balancing between teacher and hard-label supervision, where $c = 0.5$ and full distillation with $c = 1.0$ both degrade significantly from $c = 0.8$. And further tuning of this hyperparameter did not provide additional benefits, where the highest-performing distillation baseline still remains far below TARGET-SFT. This suggests that although the teacher distribution provides useful supervision, using it as a full or fixed soft target is still suboptimal.

The second ablation further confirms the importance of adaptive residual weighting. Replacing the uncertainty-dependent weight $1 - \gamma_t$ with a constant branch weight $c \in \{0.2, 0.5, 1.0\}$ gives weaker performance across settings. Although $c = 0.5$ is slightly more competitive, TARGET-SFT still achieves the highest average accuracy. This supports the main design intuition: teacher guidance should be applied more strongly when the observed token is uncertain, rather than uniformly across all tokens. Overall, the ablations validate both components of TARGET-SFT, showing that using a teacher-guided prior as a fallback mechanism in the residual branch is highly effective.

F Teacher Model Alignment

This section analyzes the alignment the model π_θ and teacher distribution π_T to better understand the effects of teacher guidance. Figure 4 visualizes the conditional distribution $P(p_T | p_\theta)$ of the teacher probability $p_T = \pi_T(\cdot | x_t)$ given the policy model probability $p_\theta = \pi_\theta(\cdot | x_t)$, both evaluated on the observed ground-truth training token y_t .

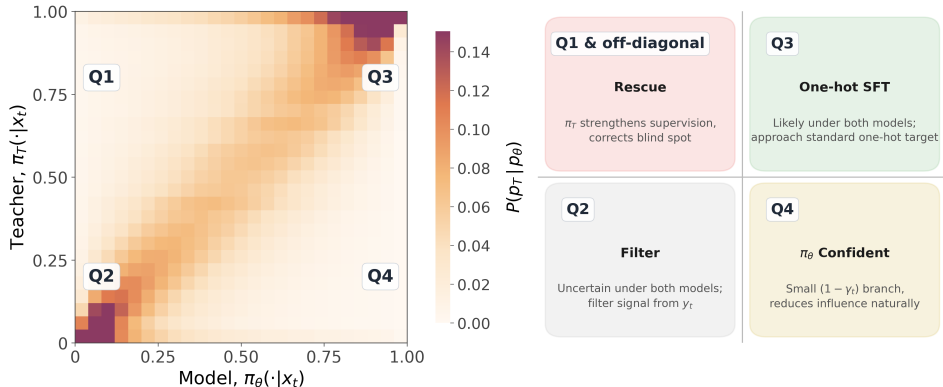


Figure 4: **Conditional Distribution of Probabilities.** This visualizes $P(p_T | p_\theta)$, the teacher probability p_T given the student probability p_θ on the observed token y_t . Each column represents a fixed p_θ bin, with color intensity showing the empirical density of p_T within that bin. The four annotated quadrants define qualitatively distinct supervision regimes.

A large portion of tokens lies near the diagonal, where both models assign similar probabilities to y_t . However, the distribution shows meaningful spread around the diagonal. This indicates useful correction signal, since even modest deviations from the diagonal are cases where the teacher’s confidence differs and thus providing signals on alternative tokens in vocabulary. While the visualization only shows the marginal probabilities on y_t for clarity, we note that the more important effect is the teacher’s full redistribution of probability mass across alternative tokens. And divergence on y_t serves as a proxy for broader differences in the teacher’s beliefs over the vocabulary, enabling fine-grained adjustments that the student’s current distribution cannot capture.

The off-diagonal density in Q1 represents stronger disagreements (high p_T , low p_θ), where teacher guidance is most informative. These tokens correspond to cases where the base model lacks confidence, but the teacher recognizes the token as plausible or important. This shows the role of teacher guidance as a fallback signal: when the student is uncertain, the teacher strengthened supervision rather than relying solely on the student’s current belief. Notably, many tokens cluster at $p_T \approx 1.0$, indicating that the teacher frequently provides strong corrections on tokens the student underweights.

In Q2 (both p_T and p_θ low), both models are uncertain about the observed token. These may correspond to noisy, idiosyncratic, or highly non-unique tokens. Standard SFT treats them as fully reliable labels, forcing exact imitation through one-hot target δ_{y_t} . In contrast, a softer target reduces imitation strength here, allowing probability mass to plausible alternatives. This helps avoid fitting dataset artifacts or arbitrary surface choices.

In Q3, the two models assign high probability to y_t . These are high-confidence tokens where the label is likely reliable and unambiguous. The target thus remains close to standard SFT one-hot δ_{y_t} , since both models support strong imitation. Finally, in Q4 (high p_θ , low p_T), the student model is already confident but the teacher is uncertain. In this case, the teacher supervision is downweighted through a smaller $1 - \gamma_t$, naturally reducing its influence.

Together, this analysis supports the motivation of TARGET-SFT, providing a selective fallback distribution to adjust the confidence on dataset tokens. It strengthens supervision when the model is uncertain, while relaxing imitation on low-confidence uncertain tokens. This provides a more adaptive alternative to standard SFT, which imposes the strict one-hot target δ_{y_t} regardless of token uncertainty or model-data alignment. Appendix G provides example trajectories showing tokens in the Q1 (high p_T , low p_θ) and Q2 (both low), ideally corresponding to useful knowledge vs. uncertain/noisy tokens.

G Qualitative Examples

Figures 6, 5, 7 show example trajectories from NuminaMath-67k dataset. **Rescue** token y_t is assigned a low probability under π_θ but high probability under π_T , hence strengthens the supervision that is otherwise weak. **Filter** token y_t has low probability under both π_θ and π_T , thus relaxing its imitation strength. Rescue tends to be answer-binding structural tokens, while Filter tends to be stylistic or chain-of-thought bridge words (e.g., *I*, *First*, *Thus*, *Therefore*, *So*, etc)

Rescue · 11 **Filter · 77** Response · 460 tokens

PROMPT

S Y S T E M
Please reason step by step, and put your final answer within `\boxed{}`.

U S E R
In year N \$, the 250^{th} day of the year is a Monday. In year $N+2$ \$, the 300^{th} day is also a Monday. Determine on what day of the week the 150^{th} day of year $N-1$ occurred.
 $(A) \text{ Tuesday} \quad (B) \text{ Wednesday} \quad (C) \text{ Thursday} \quad (D) \text{ Friday} \quad (E) \text{ Saturday}$

RESPONSE

1. **Identify given days and calculate day of the week for the adjusted years**:
 - Year N \$: 250^{th} day is Monday.
 - Year $N+2$ \$: 300^{th} day is Monday.
2. **Compute day equivalences modulo 7**:
 - Day $250 \pmod 7 = 5$ (since $250 = 35 \times 7 + 5$).
 - Day $300 \pmod 7 = 6$ (since $300 = 42 \times 7 + 6$).
3. **Adjust and determine the year type (leap or regular)**:
 - Since there are 2 days difference in modulo 7 calculations between N and $N+2$, and given that these two days are Monday, it implies a leap year must exist between N and $N+2$. Typically, this would be year $N+1$ if it is the leap year.
4. **Calculate the day for 150^{th} day of year $N-1$** :
 - Since year $N+1$ is a leap year, year $N-1$ is a regular year.
 - Day $150 \pmod 7 = 3$ (since $150 = 21 \times 7 + 3$).
 - Counting back from the 250th day of year N (Monday), the 150th day of year $N-1$ should be 100 days earlier modulo 7, i.e., $3 \pmod 7 = 3$ days earlier in the week than Monday. Counting backwards, Monday, Sunday, Saturday, Friday. Thus, the 150th day is Friday.

Conclusion with boxed answer:
 The 150^{th} day of year $N-1$ occurred on a `\text{Friday}`.
 The final answer is `\boxed{\text{Friday}}`

Figure 5: Example Trajectory #1.

Rescue · 9 Filter · 18 Response · 483 tokens

PROMPT

SYSTEM

Please reason step by step, and put your final answer within $\boxed{\}$.

USER

Given vectors \vec{a} , \vec{b} that satisfy $|\vec{a}| = 1$, $|\vec{b}| = 2$, and $\vec{a} \cdot \vec{b} = -\frac{1}{2}$, find:

1. The value of $|\vec{a} + \vec{b}|$;
2. The cosine value of the angle between \vec{a} and $\vec{b} - \vec{a}$.

RESPONSE

1. We know that $|\vec{a} + \vec{b}|^2 = |\vec{a}|^2 + 2\vec{a} \cdot \vec{b} + |\vec{b}|^2 = 1^2 + 2(-\frac{1}{2}) + 2^2 = 4$. Thus, $|\vec{a} + \vec{b}| = \boxed{2}$.

2. First, compute the dot product of \vec{a} and $\vec{b} - \vec{a}$:

$$\vec{a} \cdot (\vec{b} - \vec{a}) = \vec{a} \cdot \vec{b} - |\vec{a}|^2 = -\frac{1}{2} - 1 = -\frac{3}{2}.$$

Next, calculate the magnitude of $\vec{b} - \vec{a}$:

$$|\vec{b} - \vec{a}|^2 = |\vec{b}|^2 - 2\vec{a} \cdot \vec{b} + |\vec{a}|^2 = 2^2 - 2(-\frac{1}{2}) + 1 = 6. \text{ Thus, } |\vec{b} - \vec{a}| = \sqrt{6}.$$

Let α be the angle between \vec{a} and $\vec{b} - \vec{a}$. Then,

$$\cos \alpha = \frac{\vec{a} \cdot (\vec{b} - \vec{a})}{|\vec{a}| \cdot |\vec{b} - \vec{a}|} = \frac{-\frac{3}{2}}{1 \cdot \sqrt{6}} = -\frac{\sqrt{6}}{4}.$$

So, the cosine value of the angle between \vec{a} and $\vec{b} - \vec{a}$ is $\boxed{-\frac{\sqrt{6}}{4}}$.

Figure 6: Example Trajectory #2.

PROMPT

SYSTEM

Please reason step by step, and put your final answer within `\boxed{}`.

USER

On a board, nine quadratic trinomials are written: $x^2+a_1x+b_1, x^2+a_2x+b_2, \dots, x^2+a_9x+b_9$. It is known that the sequences (a_1, a_2, \dots, a_9) and (b_1, b_2, \dots, b_9) are arithmetic progressions. It turns out that the sum of all nine trinomials has at least one root. What is the maximum number of the original trinomials that may not have any roots?

RESPONSE

To solve this problem, we need to analyze the given quadratic trinomials and take into account the fact that their coefficients form arithmetic progressions.

1. **Define the Quadratic Polynomials:**

We have nine quadratic trinomials:

$$P_i(x) = x^2 + a_i x + b_i \quad \text{for } i = 1, 2, \dots, 9$$

where the sequences (a_1, a_2, \dots, a_9) and (b_1, b_2, \dots, b_9) are arithmetic progressions.

2. **Sum of Polynomials:**

Let's consider the sum of all nine polynomials:

$$P(x) = \sum_{i=1}^9 P_i(x) = \sum_{i=1}^9 (x^2 + a_i x + b_i)$$

Since each $P_i(x)$ contains an x^2 term and there are nine $P_i(x)$:

$$P(x) = 9x^2 + \left(\sum_{i=1}^9 a_i\right)x + \sum_{i=1}^9 b_i$$

3. **Arithmetic Properties and Symmetry:**

Because (a_i) and (b_i) are in arithmetic progression, they have symmetric properties. Specifically:

$$a_i + a_{10-i} = 2a_5 \quad \text{and} \quad b_i + b_{10-i} = 2b_5 \quad \text{for } i = 1, 2, \dots, 4$$

Thus, the sums:

$$\sum_{i=1}^9 a_i = 9a_5 \quad \text{and} \quad \sum_{i=1}^9 b_i = 9b_5$$

Therefore, the polynomial $P(x)$ becomes:

$$P(x) = 9x^2 + 9a_5 x + 9b_5 = 9(x^2 + a_5 x + b_5)$$

So, $P(x) = 9P_5(x)$.

4. **Existence of Roots:**

According to the problem, the sum $P(x)$ has at least one root. Hence, $P_5(x)$ must have at least one root x_0 :

$$P_5(x_0) = x_0^2 + a_5 x_0 + b_5 = 0$$

5. **Pairs of Polynomials:**

Notice that for any root x_0 :

$$P_i(x_0) + P_{10-i}(x_0) = 2P_5(x_0) = 0$$

This implies that for each pair (P_i, P_{10-i}) for $i = 1, 2, 3, 4$, at least one of the trinomials $P_i(x_0)$ or $P_{10-i}(x_0)$ must have a root.

6. **Counting Polynomials Without Roots:**

Since there are four pairs and one middle polynomial P_5 , at least five trinomials must have a root. Consequently, the maximum number of trinomials that do not have any roots is:

$$9 - 5 = 4$$

7. **Example Verification:**

Verifying that it is possible for exactly four trinomials not to have roots, we construct an example where five trinomials have exactly one root:

$$x^2 - 4, x^2 - 3, x^2 - 2, \dots, x^2 + 4$$

Conclusion:

Thus, the maximum number of the given trinomials that can be without any roots is:

$$\boxed{4}$$

Figure 7: Example Trajectory #3.

H Response Length

This section analyzes the relationship between the model’s output response length and its accuracy performance. Figure 8 shows the comparison on Qwen2.5-Math-1.5B for the two mathematical reasoning datasets, and Qwen2.5-1.5B for the m23k dataset.

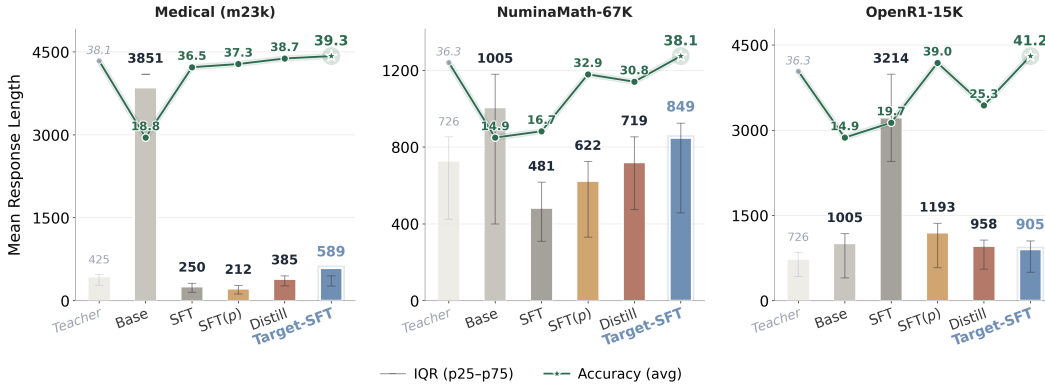


Figure 8: **Comparison of Response Length.** Bars indicate mean response length (tokens), error bars show the interquartile range (p25–p75), and the green curve reports average accuracy from evaluation in the main text. Response length does not consistently predict performance: long outputs from the base model or standard SFT often reflect rambling, repetition, or dataset-specific style imitation, while TARGET-SFT achieves strong accuracy with more moderate and stable response lengths.

On m23k and NuminaMath-67K, trained models that produce longer responses generally have higher accuracies than the shorter-output SFT variants, suggesting that the increase in reasoning length is beneficial. However, this relationship between response length and model performance is not consistent on OpenR1-15K, where standard SFT produces the longest responses but achieves substantially lower accuracy than the others. Meanwhile, TARGET-SFT achieves the highest accuracy with relatively shorter responses. This indicates that this pattern may be dataset-dependent and response length alone is not a reliable proxy for reasoning quality.

A closer inspection of model outputs suggests that the long responses from the base model often reflect poor generation behavior rather than longer reasoning. In particular, the base model occasionally shows rambling, unstable formatting, repetition, or failure to terminate properly. This inflates the average response length while yielding weak performance. In contrast, all trained models produce more consistent outputs and more stable response formats.

Standard SFT appears especially sensitive to the surface style of the training corpus. For example, on OpenR1-15K, it tends to imitate the dataset’s long chain-of-thought monologue style, closely matching its response length and tone. This observation aligns with the intuition behind SFT’s one-hot target δ_{y_t} , which applies strict supervision to every observed token in the training data. As a result, standard SFT may overfit to dataset-specific surface forms, including verbosity and stylistic structures, without necessarily improving the robustness of the underlying reasoning process.

By comparison, SFT(p), distillation, and TARGET-SFT tend to preserve more of the base model’s flexibility. Their outputs fall into a more moderate-length regime and avoid the extreme verbosity of standard SFT. These methods appear to trade some of SFT’s confident dataset-matched style for a more consistent reasoning structure that transfers better across corpora, leading to stronger accuracy without simply increasing response length or mimicking styles from the dataset.